Chem

CellPress

Article

Computationally designed ligands enable tunable borylation of remote C–H bonds in arenes

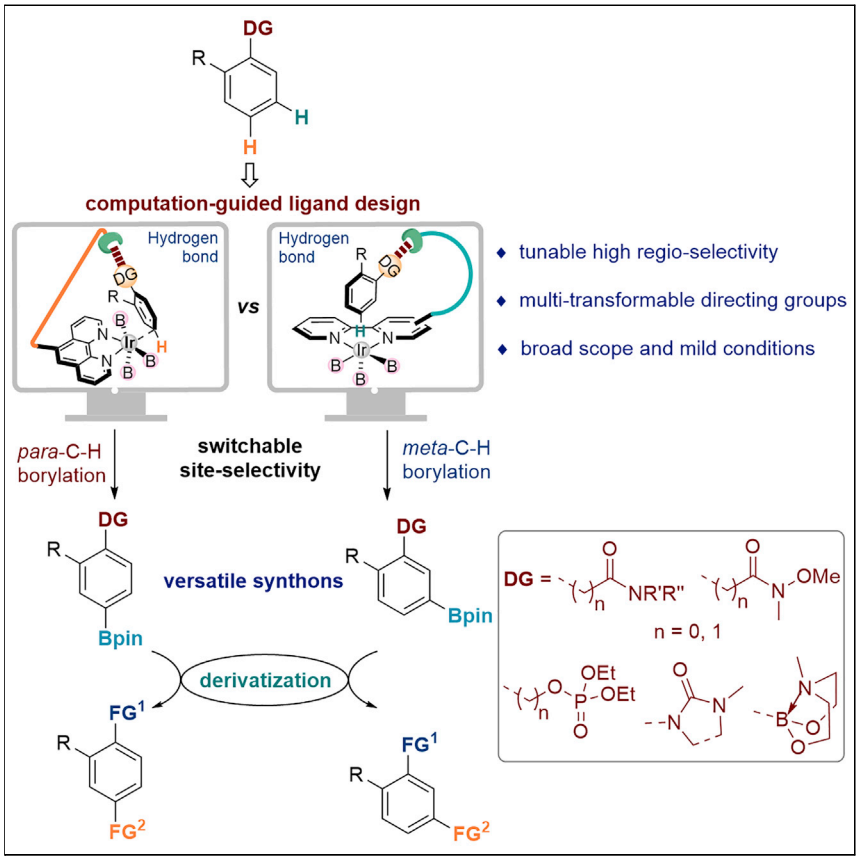

Remote selective C–H functionalization of arenes is challenging because *meta*- and *para*-C–H bonds are far away from the directing group but are adjacent with small differences in reactivity. Here, guided by DFT calculations, we designed two sets of ligands to accomplish the *meta*- and *para*-selective borylation of arenes. Various hydrogen bond acceptors can be used as multi-transformable directing groups. The tunable site selectivity and rich transformations of both directing groups and formed C–B bonds increase the diversity of multi-substituted arenes dramatically.

Wenju Chang, Yu Chen, Shuo Lu, ..., Kendall N. Houk, Fang Liu, Yong Liang

yongliang@nju.edu.cn

Highlights

Tunable *meta*- and *para*-C–H boroylation

Multi-transformable directing groups

DFT-calculations-guided ligand design

Broad substrate scope and practical gram-scale process

Chang et al., Chem *8*, 1775–1788
June 9, 2022
https://doi.org/10.1016/j.chempr.2022.04.025

Chem

CellPress

Article

Computationally designed ligands enable tunable borylation of remote C–H bonds in arenes

Wenju Chang,[1,5] Yu Chen,[1,5] Shuo Lu,[1,5] Hongyun Jiao,[1] Yajun Wang,[1] Tianyu Zheng,[1] Zhuangzhi Shi,[1] Yingbin Han,[1] Yi Lu,[1] Yi Wang,[1] Yi Pan,[1] Jin-Quan Yu,[2] Kendall N. Houk,[3] Fang Liu,[4] and Yong Liang[1,6,*]

SUMMARY

An ideal way to synthesize multi-substituted arenes is the selective installation of any group on any position of aromatic rings with any substituent. However, reactant-controlled selective functionalization of both *meta*- and *para*-C–H bonds is essentially impossible because of their intrinsically contradictory electronic and steric demands. Here, we report the first examples of catalysts that can direct the tunable borylation of a variety of arenes with precise control at either *meta* or *para* site through the computational design of ligands. A wide range of hydrogen bond acceptors can serve as directing groups, including Weinreb amides, phosphonates, and boronates, which can be easily transformed into many different types of functional groups. This work also showcases the critical role of transition-state calculations in catalyst design for remote C–H activation.

INTRODUCTION

Site-selectivity control in arene functionalization is a classic topic in synthetic chemistry. The pioneering work of Friedel and Crafts shed light on the inherent selectivity of electrophilic aromatic substitution that electrophiles attack the *ortho*- and *para*-position controlled by electron-donating substituents, whereas the electron-withdrawing substituents steer to *meta*-position under harsher conditions.[1] Additionally, increasing steric hindrance of the substituent on the aromatic ring and/or the employed reagent favors the formation of *para*-substituted arene over the *meta*- and *ortho*-substituted ones.[2,3] For a given combination of arene and reagent, it is possible to functionalize either *meta*- or *para*-C–H bond with high selectivity,[4,5] but it is essentially impossible to do both of them due to their intrinsically contradictory electronic and steric demands. The directing group strategy can override the intrinsic selectivity of substrates. In recent decades, numerous advances have been achieved for *ortho* selectivity of arenes through five- or six-membered cyclic transition states composed by substrates with directing groups and metal reagents[6] or catalysts.[7,8] Remote directing through macrocyclophane-like transition states has provided an avenue for developing *meta*- and *para*-C–H functionalizations of arenes.[9,10] The critical dependence of the site selectivity on the size and geometry of the macrocyclophane has been illustrated by well-designed templates (Figure 1A).[11,12] However, these approaches require a stoichiometric amount of complex template, which is usually covalently preinstalled on the substrate. In principle, changing the covalent bond in the cyclophane-like transition state for remote C–H activation to the noncovalent interaction may lead to the use of only a catalytic amount of ligand (Figure 1B), which will solve the problem with the highest possible atom- and step-economy.[13] This design, meanwhile, is highly challenging because

The bigger picture

The selective introduction of functional groups into the desired position of arenes with any substituent is invaluable for the diversification of aromatics. Covalently attached template strategy has provided an avenue for developing *meta*- and *para*-selective C–H functionalization of arenes. However, the design of catalyst-controlled remote C–H activation of arene remains a great challenge. Here, we report the catalyst-controlled borylation of aromatic C–H bonds *meta* or *para* to a variety of hydrogen bond acceptors through the computational design of ligands. The switchable site selectivity, various derivatization of formed C–B bonds, and late-stage transformation of directing groups into many different types of functional groups dramatically increases the diversity of multi-substituted arenes. Furthermore, the computation-guided design strategy will accelerate the discovery of new ligands or catalysts for other selective C–H functionalization.

the noncovalent interaction is much weaker than the covalent one. The transition states for both *meta*- and *para*-C–H activations involve strained cyclophane-like structures,[14,15] and the noncovalent interaction recognition site of ligands tends to disassociate to relieve strain, leading to the nondirected pathway (Figure 1B). Only ligands with the most optimal linker distance and geometry are capable of directing. In addition, *meta*- and *para*-C–H bonds are far away from the directing group but close to each other, and subtle conformation changes in transition states have a marked impact on the site selectivity. The weaker noncovalent interaction makes the transition states more flexible, increasing difficulty to differentiate reactivity between *meta* and *para* sites.

Hydrogen bonding, as an important type of noncovalent interaction, has been widely applied in the field of catalysis.[16–18] In 2015, Kanai and coworkers reported an iridium-catalyzed *meta*-C–H borylation of benzamides, in which hydrogen bond donor (urea moiety) of ligand recognizes the hydrogen bond acceptor (carbonyl group) of benzamide.[19] Various aromatic amides gave *meta* to *para* selectivity ratios from 3.3:1 to >30:1. Recently, several other *meta*-C–H borylations have been realized by noncovalent interaction between ligands and substrates.[20–26] Phipps and coworkers achieved *meta*-C−H borylation of aromatic quaternary ammonium salts[20] and arenes bearing trifluoroacetyl-protected amines[21] via ion-pair and hydrogen bonding interaction, respectively. They also developed an asymmetric *meta*-C−H borylation method through desymmetrization of geminal diaryl motif.[23] The Chattopadhyay's group reported the *meta*-C−H borylation of aniline derivatives directed by cation-π interaction[22] and electrostatic interaction.[24] However, the suitable directing groups are quite finite (e.g., *N*,*N*-dialkyl amide and quaternary ammonium cation), which are relatively inert with very limited transformation under mild conditions. Recently, *para*-selective C–H borylation has also been developed.[27–31] Chattopadhyay and coworkers designed an L-shaped ligand for *para*-C–H borylation of aromatic esters through Lewis acid and base interactions.[27] Nakao and coworkers reported a *para*-selective C–H borylation of amide and pyridine derivatives by cooperative iridium/aluminum catalysis.[29] The Phipps' group[30] and the Maleczka and Smith's group[31] independently disclosed the *para*-C–H borylation of anionic aromatics with a bulky counter cation. To our knowledge, ligand-controlled *para*-C–H borylation of arenes via hydrogen bonding recognition has not been reported. More importantly, although quite a few elegant approaches have been developed to construct *meta*- or *para*-substituted arenes,[32] tunable functionalization of both *meta*- and *para*-C–H bonds in the same substrate is very rare. Here, guided by density functional theory (DFT) calculations, we have designed two sets of ligands to accomplish the Ir-catalyzed tunable *meta*- and *para*-C–H borylation of aromatic compounds for the first time (Figure 1C). In addition, we have developed a series of multi-transformable directing groups (MTDGs), such as Weinreb amide and phosphorate, which can be converted into many other functional groups efficiently (Figure 1C). Furthermore, the boronate has been demonstrated as an effective directing group in the field of C–H activation.

RESULTS AND DISCUSSION

Design of *para*-selective ligand guided by density functional theory calculations

To design a *para*-selective ligand for iridium-catalyzed C–H borylation of benzamides via hydrogen bonding recognition, we first located the *para*-C–H activation transition state of 2-chloro-*N*,*N*-dimethylbenzamide(**1a-Me**) as a model substrate in the presence of iridium-bipyridine complex (Figures 2A and S1). It was found that the optimal distance between carbonyl O atom (hydrogen bond acceptor) in

[1]State Key Laboratory of Coordination Chemistry, Jiangsu Key Laboratory of Advanced Organic Materials, Chemistry and Biomedicine Innovation Center, School of Chemistry and Chemical Engineering, Nanjing University, Nanjing 210023, China

[2]Department of Chemistry, The Scripps Research Institute, La Jolla, San Diego, CA 92037, USA

[3]Department of Chemistry and Biochemistry, University of California, Los Angeles, Los Angeles, CA 90095, USA

[4]College of Sciences, Nanjing Agricultural University, Nanjing 210095, China

[5]These authors contributed equally

[6]Lead contact

*Correspondence: yongliang@nju.edu.cn

https://doi.org/10.1016/j.chempr.2022.04.025

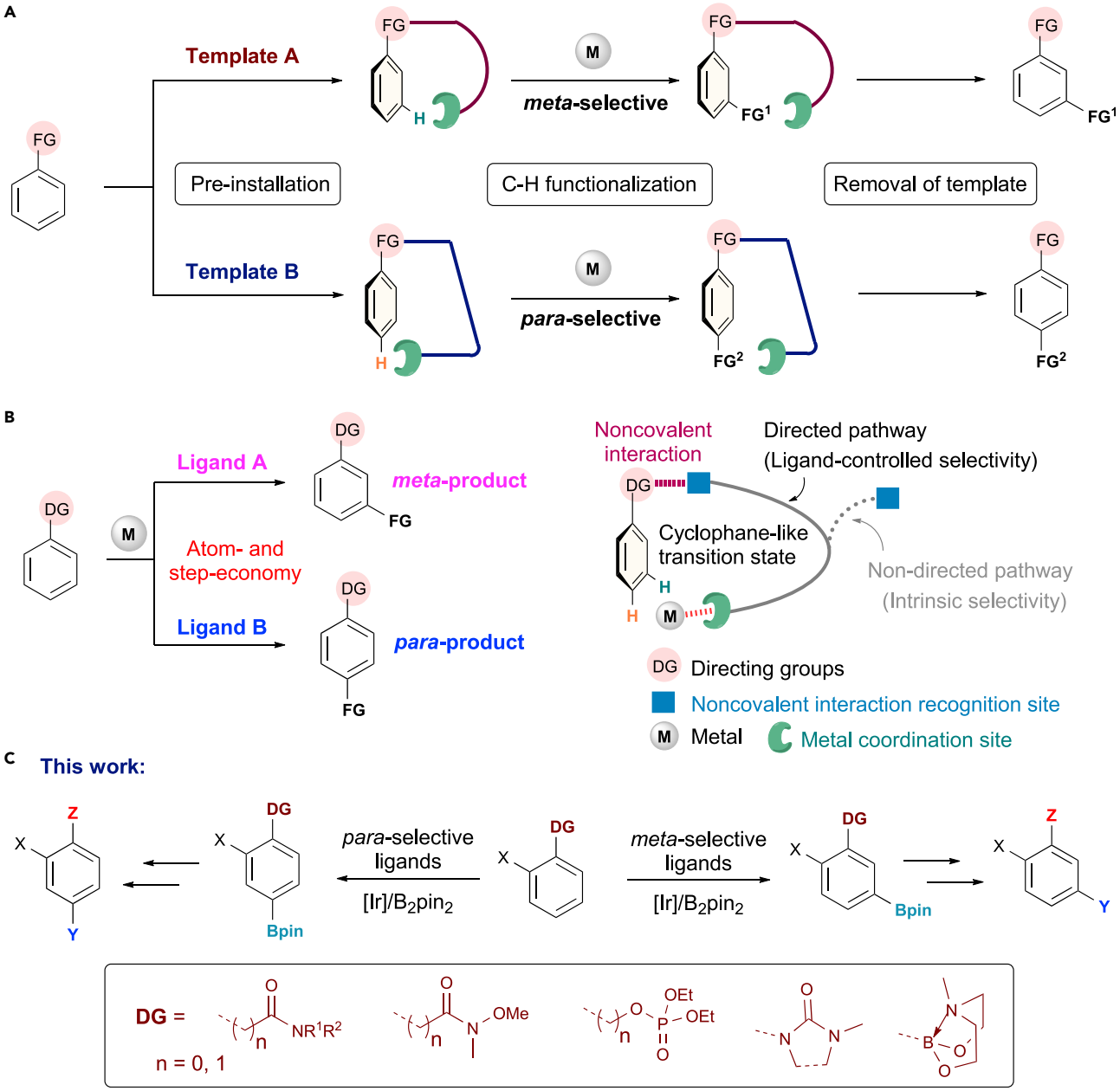

Figure 1. Directed site-selective C–H bond functionalization of arenes

(A) Template strategies.

(B) Noncovalent interaction recognition for site-selective remote C–H activation.

(C) Ligand-controlled Ir-catalyzed tunable borylation of both *meta*- and *para*-C–H bonds. B_2pin_2, bis(pinacolato)diboron.

amide **1a-Me** and iridium center is 7.1 Å, and the ideal angle between O–Ir and bipyridine plane is about 68° (Figure 2A, left). When using a 1,2-phenylene unit as the connection joint of metal coordination site and hydrogen bond donor (urea moiety), the angle between the two linkers is 60° (Figure 2A, middle). We envisioned that through choosing the right distances of two linkers, an approximately equilateral triangle shaped macrocyclophane structure could be constructed by catalyst (ligand and iridium) and amide, which would minimize the strain energy and maximize the hydrogen bonding interaction in the transition state of *para*-C–H activation. If the

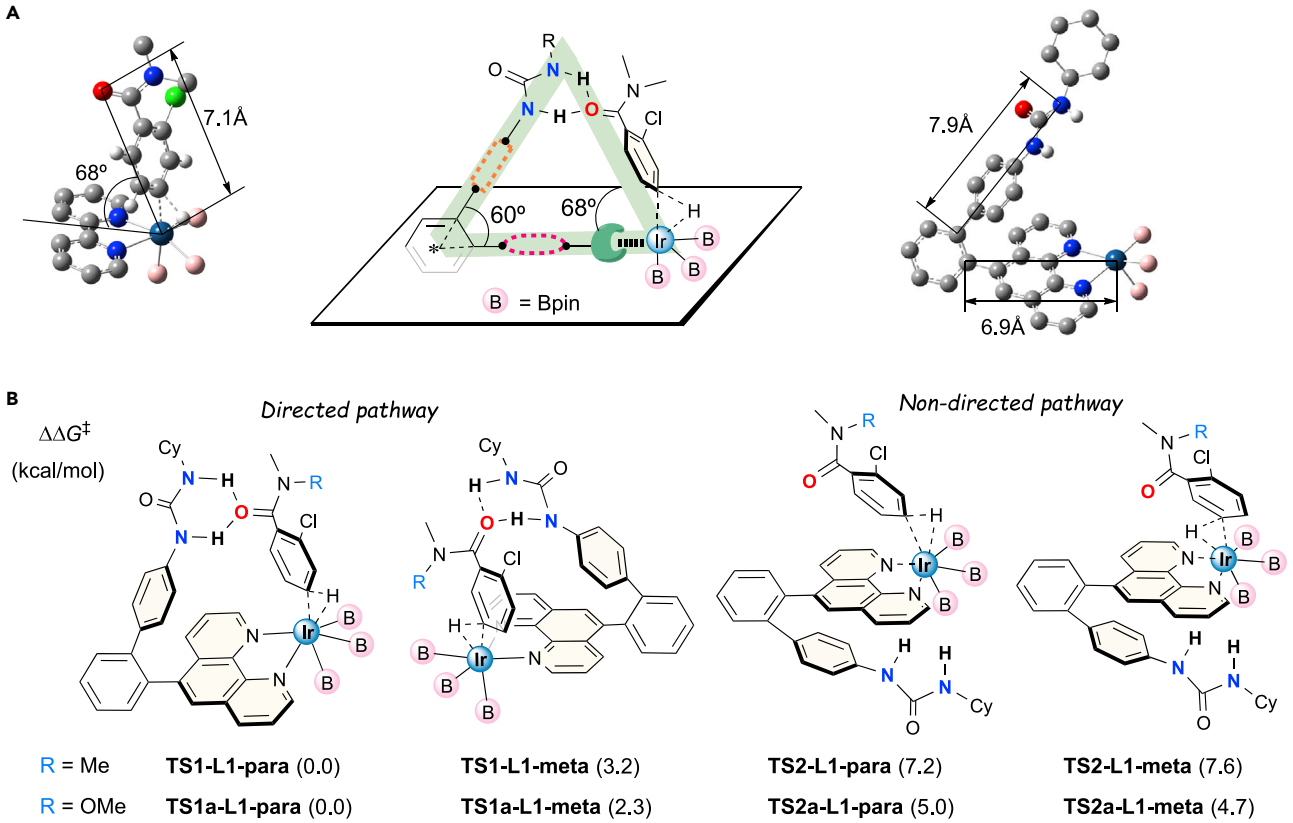

C

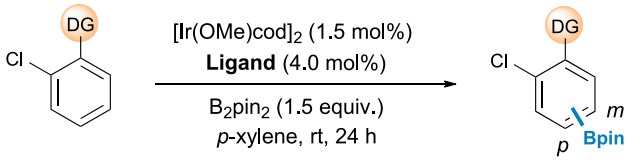

DG (*p*:*m*)	1a	9a	16a	24a
dtbpy	99% (62:38)	98% (60:40)	92% (69:31)	83% (59:41)
L1	95% (93:7)	99% (89:11)	99% (97:3)	70% (88:12)
L2	97% (93:7)	99% (92:8)	99% (98:2)	89% (94:6)
L3	98% (95:5)	76% (90:10)	99% (97:3)	83% (93:7)

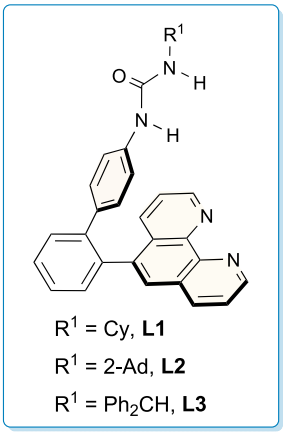

Figure 2. Computation-guided design of ligands for *para*-selective C–H borylation of arenes

(A) The design elements of *para*-selective ligand.

(B) DFT calculations for the designed ligand. The Gibbs free energies were computed with SMD(*p*-xylene)-ωB97X-D/6-311+G(d,p)[SDD for Ir]//M06/6-31G(d)[SDD for Ir].

(C) The performance of ligands in catalytic *para*-C–H borylation. Reaction conditions: substrate (0.2 mmol, 1.0 equiv), B_2pin_2 (1.5 equiv), $[Ir(OMe)cod]_2$ (1.5 mol %), and ligand (4.0 mol %). Yield values and ratios of *para* to *meta* were determined from the crude ^1H NMR spectra. dtbpy, 4,4′-di-tert-butyl-2,2′-bipyridine. Cy, cyclohexyl. 2-Ad, 2-adamantyl.

connection joint (1,2-phenylene unit) was directly introduced at the 3-position of bipyridine ligand (Figure S2), the distance between the connection joint and iridium center is 4.5 Å, which is much shorter than the desired length (about 7 Å). The

A

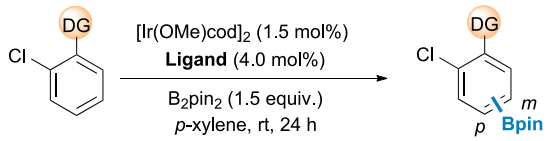

DG (m:p)	1a	9a
L4	99% (93:7)*	99% (74:26)
L5	99% (95:5)	84% (88:12)
L6	99% (97:3)	99% (97:3)
L7	96% (97:3)	90% (96:4)

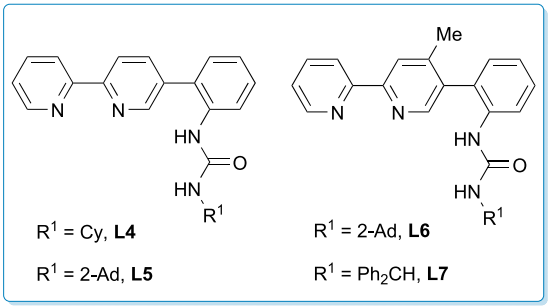

B

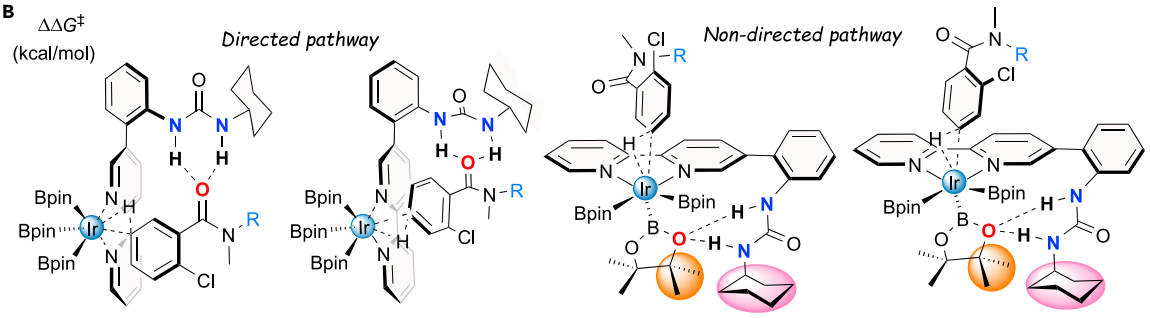

R = Me	**TS1-L4-meta** (0.0)	**TS1-L4-para** (5.4)	**TS2-L4-meta** (3.7)	**TS2-L4-para** (2.6)
R = OMe	**TS1a-L4-meta** (0.0)	**TS1a-L4-para** (5.3)	**TS2a-L4-meta** (1.5)	**TS2a-L4-para** (1.5)

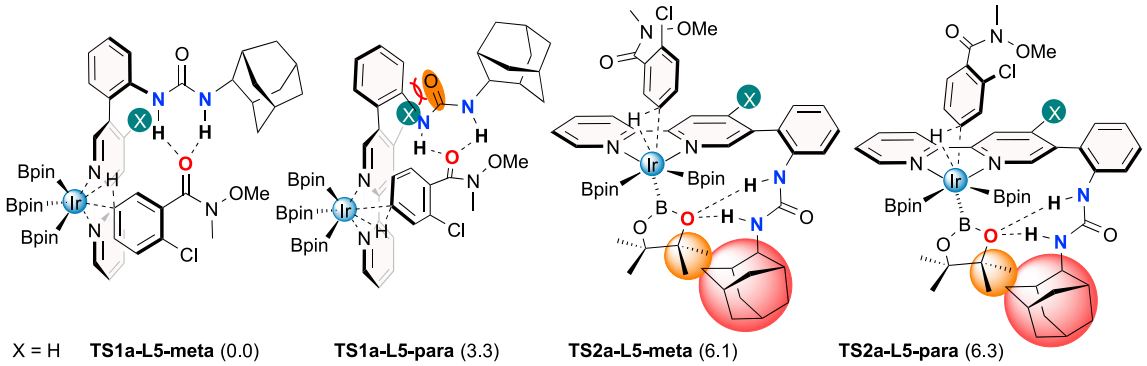

X = H	**TS1a-L5-meta** (0.0)	**TS1a-L5-para** (3.3)	**TS2a-L5-meta** (6.1)	**TS2a-L5-para** (6.3)
X = Me	**TS1a-L6-meta** (0.0)	**TS1a-L6-para** (5.1)	**TS2a-L6-meta** (6.7)	**TS2a-L6-para** (6.7)

C

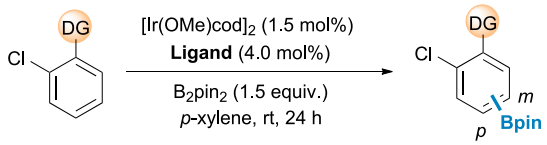

DG (m:p)	16a	24a
L4	71% (55:45)	20% (69:31)
L6	99% (95:5)	45% (93:7)
L8	99% (95:5)	99% (94:6)

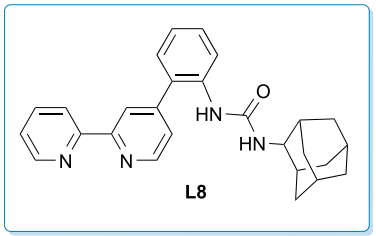

Figure 3. Computation-guided evolution of ligands for *meta*-selective C–H borylation of arenes

(A) Development of ligands for *meta*-C–H borylation of Weinreb amides.

(B) DFT insights into the ligand evolution. The Gibbs free energies were computed with SMD(*p*-xylene)-ωB97X-D/6-311+G(d,p)[SDD for Ir]//M06/6-31G(d)[SDD for Ir].

(C) Development of ligands for remote *meta*-C–H borylation. Reaction conditions: substrate (0.2 mmol, 1.0 equiv), B_2pin_2 (1.2 or 1.5 equiv), $[Ir(OMe)cod]_2$ (1.5 mol %), and ligand (4.0 mol %). Yield values and ratios of *meta* to *para* were determined from the crude ^1H NMR spectra. *Data from Kuninobu et al.[19]

iridium/phenanthroline-derived ligand system was demonstrated as a highly active alternative to the well-established iridium/bipyridine-derived ligand system.[33,34] To our delight, when bipyridyl moiety was replaced by 1,10-phenanthrolinyl moiety, the distance between the connection joint and iridium center is 6.9 Å (Figure S2), which just meets our requirements for the length of one linker. For another linker, if the urea moiety is directly attached to the connection joint, the linker length is only 3.6 Å (Figure S2). We found that the insertion of a rigid 1,4-phenylene moiety into this linker can not only fit the requirement of distance (7.9 Å, Figure 2A, right) but also reduce the flexibility of the *para*-selective transition-state structure. Further DFT calculations using this newly designed ligand **L1** demonstrated that, for amide **1a-Me**, in the directed *para*-selective pathway, the activation free energy is 3.2 kcal/mol lower than that in the *meta* one, which predicts an excellent ratio of *para* to *meta* (Figure 2B, **TS1-L1-para** versus **TS1-L1-meta**, Figure S3). Nondirected pathways, in which the urea moiety in **L1** has no hydrogen bonding with substrate, were also calculated, and they are much higher in energy than directed pathways (Figure 2B).

Initial screening of newly designed *para*-selective ligand

Aldehydes and ketones are important intermediates in organic synthesis, but they can be reduced in Ir-catalyzed borylation processes.[27] Weinreb amides serve as effective acylating agents and can be converted readily into various carbonyl compounds.[35] In spite of this great promise, a Weinreb amide-directed *para*-C–H borylation of arenes has not been documented. Our calculations predicted that for Weinreb amide **9a**, ligand **L1** is still suitable (Figures 2B and S4). Encouraged by positive results of computation, ligands **L1**-**L3** were synthesized by simple coupling reactions and the treatment with corresponding isocyanate. Subsequently, four different classes of substrates **1a**, **9a**, **16a**, and **24a** were tested in the presence of iridium with ligands **L1**-**L3**, affording good to excellent *para*-selectivity and yields (Figure 2C). This indicates that the *para*-selective ligand works just as we designed it: the geometry of ligand mainly controls selectivity. To further support this, we computed the distortion energy[36] of ligand fragment in the directed C–H activation transition states, which was found to be a significant contributor to the observed *para*-selectivity (Figure S5A).

Evolution of *meta*-selective ligand

Although Kanai's ligand **L4** has been successfully used for benzamide **1a** (m:p = 93:7, Figure 3A) in the *meta*-C–H borylation,[19] it fails to reach good *meta*-selectivity for the other three types of substrates **9a** (m:p = 74:26, Figure 3A), **16a** (m:p = 55:45, Figure 3C), and **24a** (m:p = 69:31, Figure 3C). To develop *meta*-selective ligands with better performance for more diverse substrates, we performed a series of DFT calculations using benzamide **1a-Me** (a homolog of **1a**) and Weinreb amide **9a** (Figures 3B, S6, and S7). Our calculations showed that the geometry of Kanai's ligand favors *meta*-selectivity significantly in the directed C–H activation transition states (Figure S5B). The main drawback of ligand **L4** is that in the nondirected pathways, although the urea moiety in ligand **L4** has no hydrogen bonding with amide, it recognizes the O atom in one Bpin group at iridium center via N–H···O interaction.

This makes the energies of nondirected transition states very close to those of directed ones. Although the Sunoj group reported a computational study on Kanai's work to explore the origin of *meta*-selectivity, these crucial nondirected pathways were not discovered.[37] For amide **1a-Me**, the directed *meta*-C–H activation barrier (via **TS1-L4-meta**) is 2.6 kcal/mol lower than the nondirected *para* one (via **TS2-L4-para**). Experimentally, a good *meta*-selectivity (>10:1) was still observed. However, compared with *N*,*N*-dialkylbenzamide, the Weinreb amide is a weaker hydrogen bond acceptor due to the electron-withdrawing inductive effect of the OMe group, which reduces the hydrogen bonding interaction between amide and urea by about 1 kcal/mol (Figure S8). Therefore, in the case of Weinreb amide **9a**, the energy of the directed *meta*-C–H activation (via **TS1a-L4-meta**) is only 1.5 kcal/mol lower than that of the nondirected *para* one (via **TS2a-L4-para**). This is in accordance with an obvious drop of *meta*-selectivity (from 93:7 to 74:26, Figure 3A).

We envisioned that the introduction of a bulky group (such as 2-adamantyl) into the urea moiety would increase the repulsion between the Bpin at iridium center and the urea in ligand to inhibit nondirected pathways. This is supported by our DFT calculations (Figures 3B and S9) and subsequent experiments using ligand **L5**, in which the ratio of *meta* to *para* is improved to 95:5 for **1a** and 88:12 for **9a**, respectively (Figure 3A). In addition, after analyzing the geometry of ligand **L5** in two directed transition states, we found that in the directed *para*-C–H activation transition state **TS1a-L5-para**, the carbonyl group of urea is very close to the 4-position of bipyridine skeleton (shown as X, Figures 3B and S9). Inspired by this, ligand **L5** (X = H) is evolved to ligand **L6** (X = Me, Figure 3A) with the purpose of increasing the steric hindrance to further disfavor the directed *para*-C–H activation. Subsequent calculations with ligand **L6** predicted an excellent *meta*-selectivity (>100:1, X = Me, Figures 3B and S10). It is notable that the Kuninobu group also observed a methyl effect on the reaction rate of the *meta*-selective borylation by introducing a methyl group on the 1,2-phenylene moiety.[38] When we tested ligand **L6**, both amide **1a** and Weinreb amide **9a** gave a 97:3 ratio of *meta* to *para* (Figure 3A). For the phenylacetic acid-derived amide **16a** and Weinreb amide **24a**, ligand **L6** also dramatically improved the *meta*-selectivity (from 55: 45 to 95:5 & from 69:31 to 93:7, respectively), although it gave a moderate yield for **24a** (Figure 3C). Finally, ligand **L8**, which moved the phenyl group from 5-position to 4-position of bipyridine (Figure 3C), improved reactivity efficiently (99% yield) and retained the outstanding *meta*-selectivity (94:6 for **24a**, Figure 3C). This shows that the redesigned *meta*-selective ligands **L6**-**L8** can effectively block both nondirected and directed *para*-selective pathways, leading to excellent performance with broad substrate scope.

Substrate scope

With both *para*-selective ligands **L1**-**L3** and *meta*-selective ligands **L6**-**L8** in hand, we surveyed the substrate scope of the tunable site-selective C–H borylation (Figure 4). For the *ortho*-substituted benzamides, both *meta*-isomers **1b**-**4b** and *para*-isomers **1c**-**4c** were obtained with high regioselectivity and yields. In the case of unsubstituted benzamide **5a**, *meta*- or *para*-product **5b** or **5c** was predominantly generated using the corresponding ligand **L6** or **L3**, whereas **L6** gave a moderate yield for **5b** due to the competitive formation of di-*meta*-borylated product. For 3-F substituted amide **6a**, when ligand **L6** was used, the *meta*-borylated product **6b** was formed with 96:4 regioselectivity and 89% isolated yield. The complementary *para*-C–H borylation process can be achieved using **L3**, giving **6c** with a 97:3 ratio of *para* to *meta*. Isoindolinone derivative **7a** delivered **7b** (m:p = 97:3) and **7c** (p:m = 98:2) with **L7** and **L2**, respectively. We also examined picolinamide **8a**, which exhibited excellent

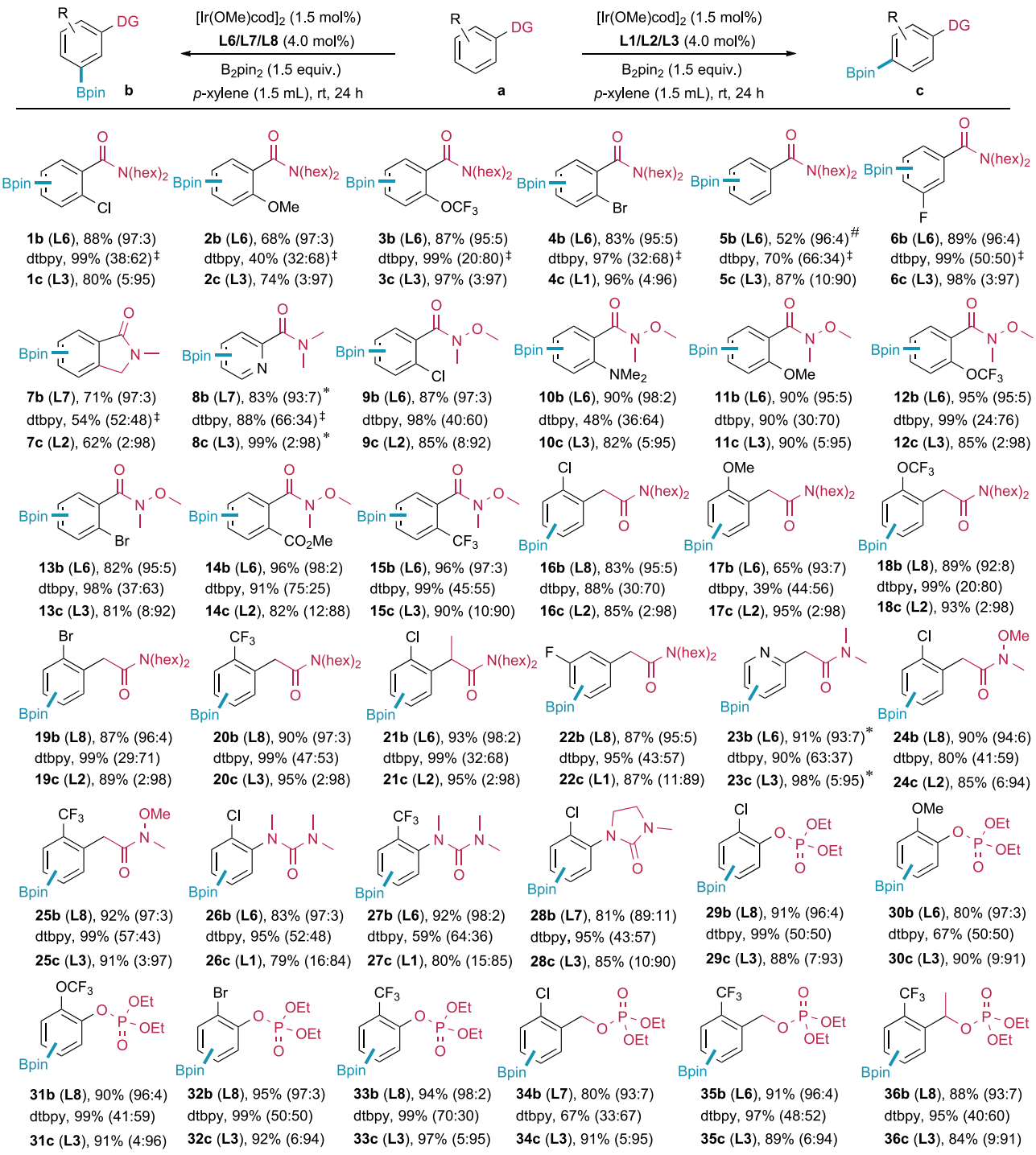

Figure 4. Substrate scope of the tunable borylation of *meta*- and *para*-C–H bonds in arenes

Reaction conditions: substrate (0.2 or 1.0 mmol, 1.0 equiv), B_2pin_2 (1.2 or 1.5 equiv), $[Ir(OMe)cod]_2$ (0.1 mol %–1.5 mol %), and ligand (0.3 mol %–4.0 mol %), *p*-xylene, room temp, 24 h, see supplemental information for details. Yield and selectivity are described as follows: isolated yields (top row and bottom row); ^{1}H NMR yields of the mixture of *meta*- and *para*-products (middle row); all ratios of *meta* to *para* were determined from crude ^{1}H NMR spectra. ‡Data from Kuninobu et al.[19] #Additional 30% di-*meta*-borylated product. *^{1}H NMR yields.

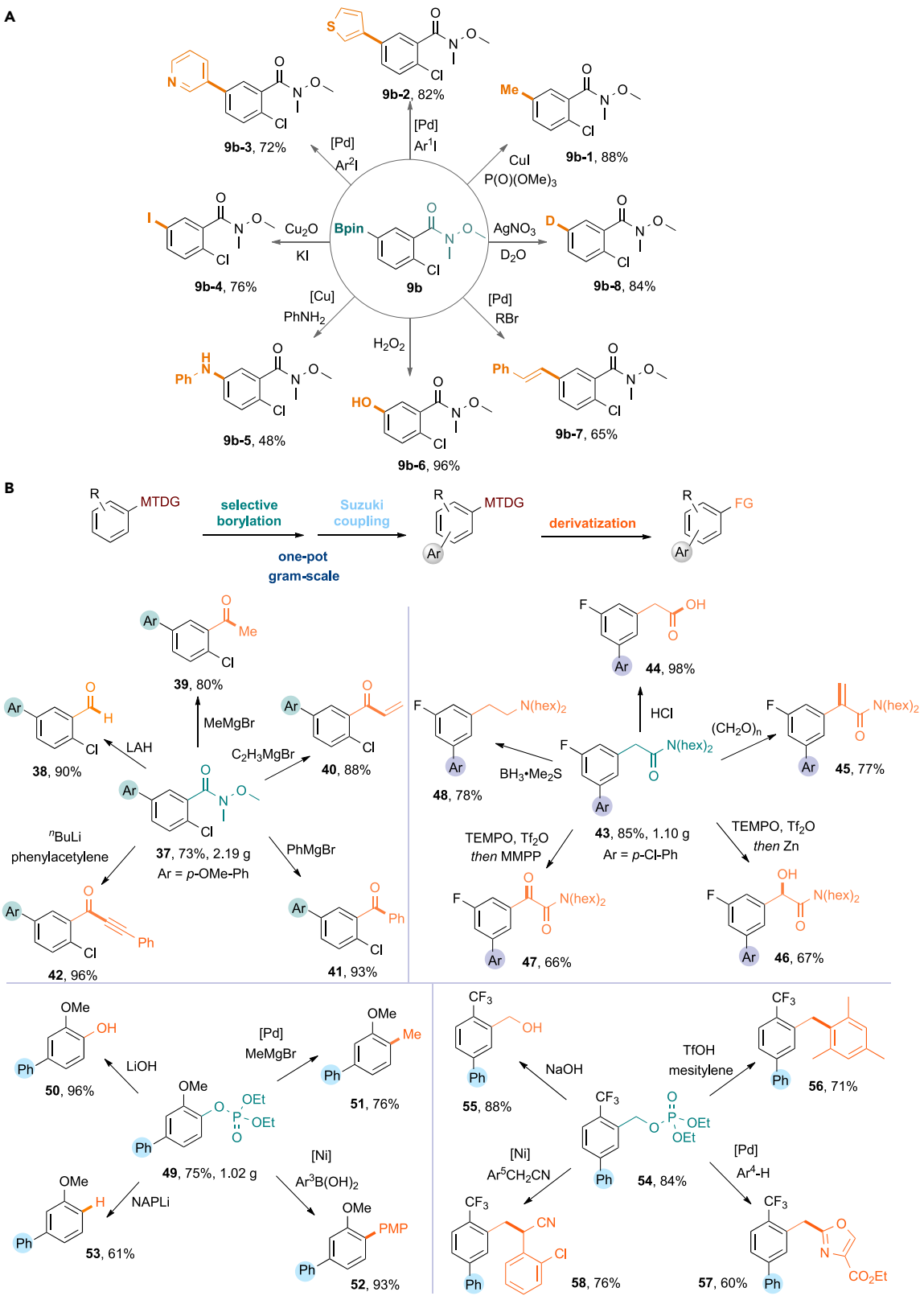
A
9b-2, 82%
9b-3, 72%
9b-1, 88%
9b-4, 76%
9b
9b-8, 84%
9b-5, 48%
9b-6, 96%
9b-7, 65%
[Pd] Ar2I
[Pd] Ar1I
CuI P(O)(OMe)3
Cu2O KI
AgNO3 D2O
[Cu] PhNH2
H2O2
[Pd] RBr
B
MTDG
selective borylation
Suzuki coupling
one-pot gram-scale
derivatization
FG
39, 80%
38, 90%
40, 88%
37, 73%, 2.19 g Ar = p-OMe-Ph
42, 96%
41, 93%
44, 98%
48, 78%
43, 85%, 1.10 g Ar = p-Cl-Ph
45, 77%
47, 66%
46, 67%
50, 96%
49, 75%, 1.02 g
51, 76%
53, 61%
52, 93%
55, 88%
54, 84%
56, 71%
58, 76%
57, 60%

Figure 5. Synthetic applications

(A) Transformations of the formed C–B bond.

(B) Conversions of multi-transformable directing groups. Yield values refer to isolated yields. TEMPO, 2,2,6,6-tetramethylpiperidin-1-oxyl; MMPP, magnesium monoperphthalate hexahydrate; NAPLi, lithium naphthalenide.

regioselectivity of **8b** (m:p = 93:7) and **8c** (p:m = 98:2). For Weinreb benzamides, both electron-rich and electron-poor groups are suitable at the 2-position of aromatic rings, giving the desired *meta*- and *para*-borylated products (**9b**-**15b** and **9c**-**15c**) with high reactivity and selectivity. The substrate **10a**, containing a Lewis basic site, also has an excellent performance without catalyst poisoning. It is noteworthy that for the aromatic ring containing both amide and ester groups, the amide-directed products **14b** and **14c** were obtained.

For various phenylacetic acid-derived amides (**16a**-**25a**), good to excellent *meta*-selectivity was observed with ligands **L6** and **L8** as well as **L1**-**L3** for *para*-selectivity. α-Methylphenylacetic acid-derived amide **21a** exhibited remarkably high site-selectivity and reactivity in both cases with **L6** and **L2**. In addition, the pyridine derivative **23a** also performed well, giving **23b** (m:p = 93:7) and **23c** (p:m = 95:5). Aniline and phenol derivatives (**26a**-**33a**) were also investigated, which are analogous to phenylacetic acid derivatives in topological features. Again, the desired both *meta*- and *para*-borylated products can be synthesized in good yields with good to excellent selectivity. We also explored the tunable site-selective C–H borylation of benzyl alcohol derivatives **34a**-**36a**, in which the functionalized C–H bond is six or seven bonds away from hydrogen bond acceptor. Gratifyingly, the desired *meta*-isomers **34b**-**36b** and *para*-isomers **34c**-**36c** were obtained with good selectivity.

Gram-scale synthesis and transformations of the formed boryl group and MTDG

This site-selective borylation process can be easily carried out in gram scale with a minimum iridium catalyst loading of 0.1 mol %. Because of the virtues of the organoboron chemistry,[39–43] the generated C–B bond can be converted into many different types of chemical bonds in one step under mild reaction conditions (Figures 5A and S11). To showcase the role of MTDG in the borylated products, we synthesized arenes **37**, **43**, **49**, and **54** in a one-pot fashion through borylation and sequential Suzuki cross-coupling (Figures 5B and S12–S15). The Weinreb amide **37** can be conveniently transformed to aldehyde **38** and a variety of ketones **39**–**42**. From amide **43**, the substituted phenylacetic acid **44** was formed in 98% yield via hydrolysis, and α,β-unsaturated amide **45** was obtained in 77% yield through a methylenation.[44] A flexible and chemoselective oxidation[45] afforded α-hydroxy amide **46** and α-keto amide **47**, respectively. The reduction with $BH_3 \cdot Me_2S$ led to the formation of the corresponding tertiary amine **48** in good yield. Treatment of phosphonate **49** with LiOH gave free phenol **50**. It should be emphasized that, in the presence of palladium[46] or nickel[47] catalysts and suitable coupling partners, arenes **51**–**52** with the phenyl or methyl substituent can be obtained efficiently. This gives an alternative solution to selective functionalization of simple aryl and alkyl substituted arenes, which are usually incapable of directing. Besides, the directing phosphonate group can be removed by lithium naphthalenide (NAPLi) to generate *meta*-substituted anisole **53**. Moreover, phosphonate **54** underwent hydrolysis or coupled with mesitylene,[48] ethyl oxazole-4-carboxylate,[49] and 2-chlorobenzyl cyanide[50] to provide corresponding products **55**–**58**. The rich transformations of the formed boryl group and MTDG, coupled with tunable *meta*- or *para*-selectivity, are expected to dramatically expand the chemical space[51] of multi-substituted arenes.

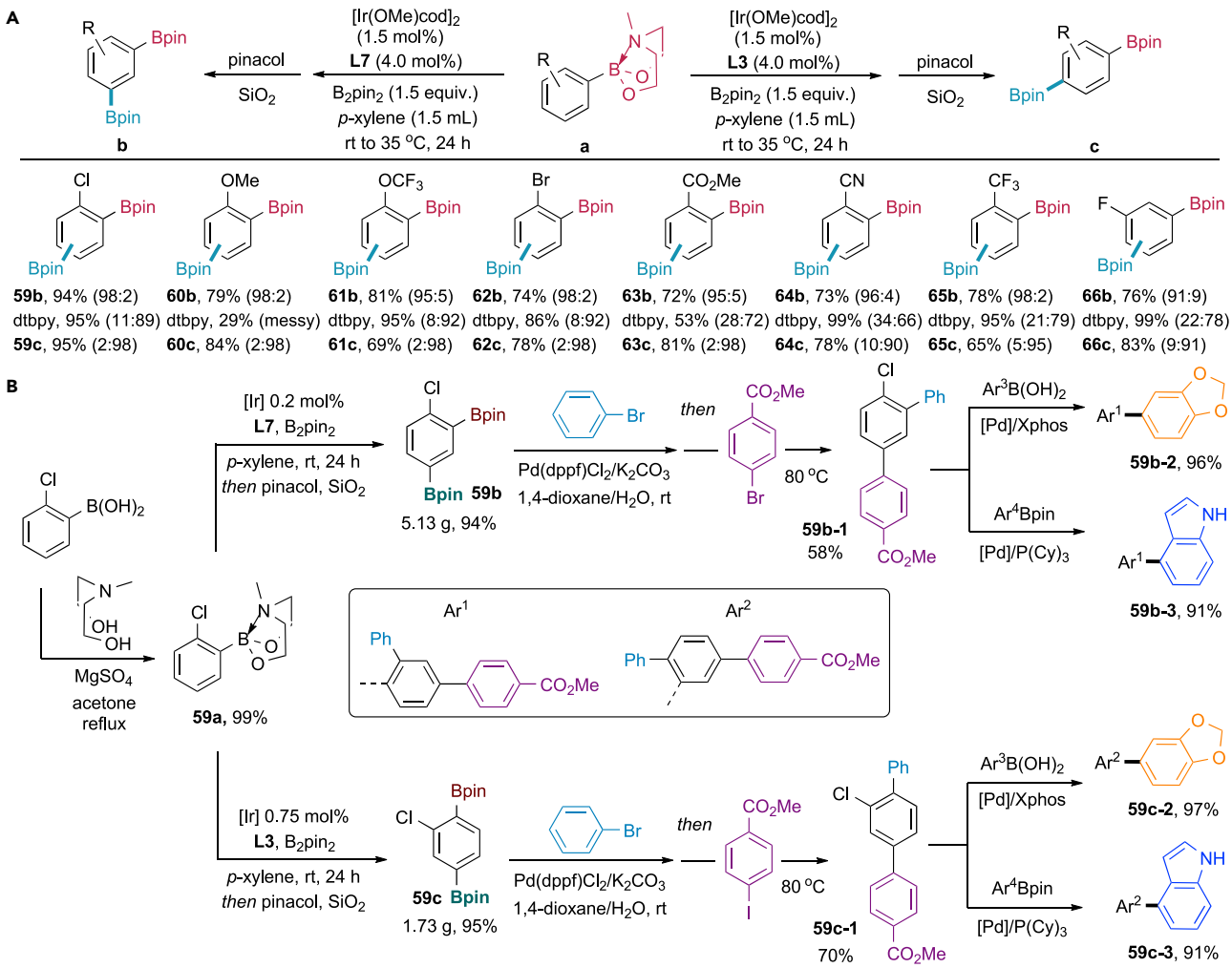

Figure 6. Boronate-directed remote C–H functionalization

(A) Substrate scope of aryl boronates. Yield and selectivity are described as follows: isolated yields (top row and bottom row); ^{1}H NMR yields of the mixture of *meta*- and *para*-products (middle row); all ratios of *meta* to *para* were determined from crude ^{1}H NMR spectra.

(B) Site-selective sequential couplings of 1,3-diBpin and 1,4-diBpin arenes. Yield values refer to isolated yields.

Arylboronate-directed tunable C–H borylation and site-selective sequential couplings

The existence of hydrogen bonding between the Bpin group and urea moiety in the nondirected pathway (Figure 3B) suggests that boronates could be employed as directing groups. To our knowledge, the boronate-directed C–H activation via hydrogen bonding recognition has not been reported, although Smith and Chirik groups reported the *para*-preference for the borylation of arylboronates.[52,53] After a few experimental tests, we found that compared with Bpin, *N*-coordinated boronate[54] can act as a stronger hydrogen bond acceptor to achieve site-selective borylation (Figures 6A and S16). The *N*-coordinated boronates **59a-66a** behave superbly in the presence of *meta*-selective ligand **L7** or *para*-selective ligand **L3**. The *N*-methyldiethanolamine was found to be a semistable-directing group and was replaced by pinacol conveniently following the borylation procedure. Various 1,3-diBpin (**59b-66b**) or 1,4-diBpin (**59c-66c**) arenes were generated in excellent selectivity and yields. As shown in Figure 6B, this reaction can be easily scaled up to a few grams. Due to the different steric environments of two Bpins in **59b** or

59c, sequential site-selective Suzuki coupling reactions can be achieved in one pot effectively. The unreacted C–Cl bond in **59b-1** or **59c-1** can then be coupled with other organoboryl compounds to deliver diverse 1,2,4-trisubstituted arenes with precise site control.

Conclusion

In summary, this work presents an approach to the precise control of both *meta*- and *para*-selectivity in arene functionalization for the first time. On the one hand, changing the covalent bond in the cyclophane-like transition state for remote C–H activation to the noncovalent interaction makes the use of a catalytic amount of ligand possible, increasing the atom- and step-economy in synthetic processes; on the other hand, computation-guided design strategy greatly accelerates the discovery of new ligands to make the desired chemistry successful, reducing the trial and error in the design and development processes.

EXPERIMENTAL PROCEDURES

Resource availability

Lead contact

Further information and requests for resources should be directed to and will be fulfilled by the lead contact, Yong Liang (yongliang@nju.edu.cn).

Materials availability

All materials generated in this study are available from the lead contact without restriction.

Data and code availability

All data are available in the manuscript or the supplementary materials. Metrical parameters for the structures of **13b, 15b, 29b, 25b, 59b-1, 35b, L6, L7, L8, 26c, 25c, 14c, 10c, 8c-Ph, and L3** are available free of charge from the Cambridge Crystallographic Data Centre (https://www.ccdc.cam.ac.uk/) under reference numbers CCDC 1921902, 1922569–1922571, 2015233, 2015234, 2015458–2015460, and 2039997–2040002, respectively.

Methods

Full experimental procedures are provided in the supplemental information.

SUPPLEMENTAL INFORMATION

Supplemental information can be found online at https://doi.org/10.1016/j.chempr.2022.04.025.

ACKNOWLEDGMENTS

This work was financially supported by the Fundamental Research Funds for the Central Universities (020514380253), the Natural Science Foundation of Jiangsu Province (BK20211555), and the Jiangsu Innovation & Entrepreneurship Talents Plan in China. We thank Dr. Yue Zhao (Nanjing University) for his assistance in crystal structure refinement. We thank the High Performance Computing Center (HPCC) of Nanjing University for doing the numerical calculations in this paper on its blade cluster system.

AUTHOR CONTRIBUTIONS

Y. Liang conceived and supervised the project. W.C. and Y. Liang wrote the paper. W.C., S.L., H.J., Yajun Wang, T.Z., and Y.H. performed the experiments. Y.C.

performed the DFT calculations. Z.S., Y. Lu, Yi Wang, Y.P., J.-Q.Y., K.N.H., and F.L. discussed the results.

DECLARATION OF INTERESTS

The authors declare no competing interests.

Received: September 6, 2021
Revised: December 6, 2021
Accepted: April 27, 2022
Published: May 23, 2022

REFERENCES

1. Calloway, N.O. (1935). The Friedel-Crafts syntheses. Chem. Rev. *17*, 327–392. https://doi.org/10.1021/cr60058a002.

2. Saito, Y., Segawa, Y., and Itami, K. (2015). para-C–H borylation of benzene derivatives by a bulky iridium catalyst. J. Am. Chem. Soc. *137*, 5193–5198. https://doi.org/10.1021/jacs.5b02052.

3. Saito, Y., Yamanoue, K., Segawa, Y., and Itami, K. (2020). Selective transformation of strychnine and 1,2-disubstituted benzenes by C–H borylation. Chem *6*, 985–993. https://doi.org/10.1016/j.chempr.2020.02.004.

4. Berger, F., Plutschack, M.B., Riegger, J., Yu, W., Speicher, S., Ho, M., Frank, N., and Ritter, T. (2019). Site-selective and versatile aromatic C–H functionalization by thianthrenation. Nature *567*, 223–228. https://doi.org/10.1038/s41586-019-0982-0.

5. Phipps, R.J., and Gaunt, M.J. (2009). A meta-selective copper-catalyzed C–H bond arylation. Science *323*, 1593–1597. https://doi.org/10.1126/science.1169975.

6. Snieckus, V. (1990). Directed Ortho metalation. Tertiary amide and O-carbamate directors in synthetic strategies for polysubstituted aromatics. Chem. Rev. *90*, 879–933. https://doi.org/10.1021/cr00104a001.

7. Colby, D.A., Bergman, R.G., and Ellman, J.A. (2010). Rhodium-catalyzed C-C bond formation via heteroatom-directed C–H bond activation. Chem. Rev. *110*, 624–655. https://doi.org/10.1021/cr900005n.

8. Lyons, T.W., and Sanford, M.S. (2010). Palladium-catalyzed ligand-directed C–H functionalization reactions. Chem. Rev. *110*, 1147–1169. https://doi.org/10.1021/cr900184e.

9. Leow, D., Li, G., Mei, T.-S., and Yu, J.-Q. (2012). Activation of remote meta-C–H bonds assisted by an end-on template. Nature *486*, 518–522. https://doi.org/10.1038/nature11158.

10. Bag, S., Patra, T., Modak, A., Deb, A., Maity, S., Dutta, U., Dey, A., Kancherla, R., Maji, A., Hazra, A., et al. (2015). Remote para-C–H functionalization of arenes by a D-shaped biphenyl template-based assembly. J. Am. Chem. Soc. *137*, 11888–11891. https://doi.org/10.1021/jacs.5b06793.

11. Meng, G., Lam, N.Y.S., Lucas, E.L., Saint-Denis, T.G., Verma, P., Chekshin, N., and Yu, J.-Q. (2020). Achieving site-selectivity for C–H activation processes based on distance and geometry: a carpenter's approach. J. Am. Chem. Soc. *142*, 10571–10591. https://doi.org/10.1021/jacs.0c04074.

12. Dey, A., Sinha, S.K., Achar, T.K., and Maiti, D. (2019). Accessing remote meta- and para-C(sp2)–H bonds with covalently attached directing groups. Angew. Chem. Int. Ed. Engl. *58*, 10820–10843. https://doi.org/10.1002/anie.201812116.

13. Zimmerman, J.B., Anastas, P.T., Erythropel, H.C., and Leitner, W. (2020). Designing for a green chemistry future. Science *367*, 397–400. https://doi.org/10.1126/science.aay3060.

14. Yang, Y.-F., Cheng, G.-J., Liu, P., Leow, D., Sun, T.-Y., Chen, P., Zhang, X., Yu, J.-Q., Wu, Y.-D., and Houk, K.N. (2014). Palladium-catalyzed meta-selective C–H bond activation with a nitrile-containing template: computational study on mechanism and origins of selectivity. J. Am. Chem. Soc. *136*, 344–355. https://doi.org/10.1021/ja410485g.

15. Maji, A., Dahiya, A., Lu, G., Bhattacharya, T., Brochetta, M., Zanoni, G., Liu, P., and Maiti, D. (2018). H-bonded reusable template assisted para-selective ketonisation using soft electrophilic vinyl ethers. Nat. Commun. *9*, 3582. https://doi.org/10.1038/s41467-018-06018-2.

16. Schreiner, P.R. (2003). Metal-free organocatalysis through explicit hydrogen bonding interactions. Chem. Soc. Rev. *32*, 289–296. https://doi.org/10.1039/b107298f.

17. Doyle, A.G., and Jacobsen, E.N. (2007). Small-molecule H-bond donors in asymmetric catalysis. Chem. Rev. *107*, 5713–5743. https://doi.org/10.1021/cr068373r.

18. Zhang, Z., and Schreiner, P.R. (2009). (Thio)urea organocatalysis-What can be learnt from anion recognition? Chem. Soc. Rev. *38*, 1187–1198. https://doi.org/10.1039/b801793j.

19. Kuninobu, Y., Ida, H., Nishi, M., and Kanai, M. (2015). A meta-selective C–H borylation directed by a secondary interaction between ligand and substrate. Nat. Chem. *7*, 712–717. https://doi.org/10.1038/nchem.2322.

20. Davis, H.J., Mihai, M.T., and Phipps, R.J. (2016). Ion pair-directed regiocontrol in transition-metal catalysis: a meta-selective C–H borylation of aromatic quaternary ammonium salts. J. Am. Chem. Soc. *138*, 12759–12762. https://doi.org/10.1021/jacs.6b08164.

21. Davis, H.J., Genov, G.R., and Phipps, R.J. (2017). meta-Selective C–H borylation of benzylamine-, phenethylamine-, and phenylpropylamine-derived amides enabled by a single anionic ligand. Angew. Chem. Int. Ed. Engl. *56*, 13351–13355. https://doi.org/10.1002/anie.201708967.

22. Bisht, R., Hoque, M.E., and Chattopadhyay, B. (2018). Amide effects in C–H activation: noncovalent interactions with L-shaped ligand for meta borylation of aromatic amides. Angew. Chem. Int. Ed. Engl. *57*, 15762–15766. https://doi.org/10.1002/anie.201809929.

23. Genov, G.R., Douthwaite, J.L., Lahdenperä, A.S.K., Gibson, D.C., and Phipps, R.J. (2020). Enantioselective remote C–H activation directed by a chiral cation. Science *367*, 1246–1251. https://doi.org/10.1126/science.aba1120.

24. Chaturvedi, J., Haldar, C., Bisht, R., Pandey, G., and Chattopadhyay, B. (2021). Meta selective C–H borylation of sterically biased and unbiased substrates directed by electrostatic interaction. J. Am. Chem. Soc. *143*, 7604–7611. https://doi.org/10.1021/jacs.1c01770.

25. Kuroda, Y., and Nakao, Y. (2019). Catalyst-enabled site-selectivity in the iridium-catalyzed C-H borylation of arenes. Chem. Lett. *48*, 1092–1100. https://doi.org/10.1246/cl.190372.

26. Kuninobu, Y., and Torigoe, T. (2020). Recent progress of transition metal-catalysed regioselective C–H transformations based on noncovalent interactions. Org. Biomol. Chem. *18*, 4126–4134. https://doi.org/10.1039/d0ob00703j.

27. Hoque, M.E., Bisht, R., Haldar, C., and Chattopadhyay, B. (2017). Noncovalent interactions in Ir-catalyzed C–H activation: L-shaped ligand for para-selective borylation of aromatic esters. J. Am. Chem. Soc. *139*, 7745–7748. https://doi.org/10.1021/jacs.7b04490.

28. Sasmal, S., Dutta, U., Lahiri, G.K., and Maiti, D. (2020). Transition metals and transition metals/lewis acid cooperative catalysis for directing group assisted para-C–H functionalization. Chem. Lett. *49*, 1406–1420. https://doi.org/10.1246/cl.200500.

29. Yang, L., Semba, K., and Nakao, Y. (2017). para-Selective C–H borylation of (hetero)arenes by cooperative iridium/aluminum catalysis. Angew. Chem. Int. Ed. Engl. *56*, 4853–4857. https://doi.org/10.1002/anie.201701238.

30. Mihai, M.T., Williams, B.D., and Phipps, R.J. (2019). Para-selective C–H borylation of common arene building blocks enabled by ion-pairing with a bulky countercation. J. Am. Chem. Soc. *141*, 15477–15482. https://doi.org/10.1021/jacs.9b07267.

31. Montero Bastidas, J.R., Oleskey, T.J., Miller, S.L., Smith, M.R., and Maleczka, R.E. (2019). Para-selective, iridium-catalyzed C–H borylations of sulfated phenols, benzyl alcohols, and anilines directed by ion-pair electrostatic interactions. J. Am. Chem. Soc. *141*, 15483–15487. https://doi.org/10.1021/jacs.9b08464.

32. Dutta, U., Maiti, S., Bhattacharya, T., and Maiti, D. (2021). Arene diversification through distal C(sp2)-H functionalization. Science *372*, esbd5992. https://doi.org/10.1126/science.

33. Seechurn, C.C.C.J., Sivakumar, V., Satoskar, D., and Colacot, T.J. (2014). Iridium-catalyzed C−H borylation of heterocycles using an overlooked 1,10-phenanthroline ligand: reinventing the catalytic activity by understanding the solvent-assisted neutral to cationic switch. Organometallics *33*, 3514–3522. https://doi.org/10.1021/om500420d.

34. Larsen, M.A., and Hartwig, J.F. (2014). Iridium-catalyzed C−H borylation of heteroarenes: scope, regioselectivity, application to late-stage functionalization, and mechanism. J. Am. Chem. Soc. *136*, 4287–4299. https://doi.org/10.1021/ja412563e.

35. Nahm, S., and Weinreb, S.M. (1981). N-methoxy-N-methylamides as effective acylating agents. Tetrahedron Lett. *22*, 3815–3818. https://doi.org/10.1016/S0040-4039(01)91316-4.

36. Bickelhaupt, F.M., and Houk, K.N. (2017). Analyzing reaction rates with the distortion/interaction-activation strain model. Angew. Chem. Int. Ed. Engl. *56*, 10070–10086. https://doi.org/10.1002/anie.201701486.

37. Unnikrishnan, A., and Sunoj, R.B. (2019). Insights into the role of noncovalent interactions in distal functionalization of the aryl C(sp2)-H bond. Chem. Sci. *10*, 3826–3835. https://doi.org/10.1039/c8sc05335a.

38. Lu, X., Yoshigoe, Y., Ida, H., Nishi, M., Kanai, M., and Kuninobu, Y. (2019). Hydrogen bond-accelerated meta-selective C−H borylation of aromatic compounds and expression of functional group and substrate specificities. ACS Catal. *9*, 1705–1709. https://doi.org/10.1021/acscatal.8b05005.

39. Mkhalid, I.A.I., Barnard, J.H., Marder, T.B., Murphy, J.M., and Hartwig, J.F. (2010). C–H activation for the construction of C-B bonds. Chem. Rev. *110*, 890–931. https://doi.org/10.1021/cr900206p.

40. Suzuki, A. (2011). Cross-coupling reactions of organoboranes: an easy way to construct C-C bonds (Nobel Lecture). Angew. Chem. Int. Ed. Engl. *50*, 6722–6737. https://doi.org/10.1002/anie.201101379.

41. Lv, J., Chen, X., Xue, X.-S., Zhao, B., Liang, Y., Wang, M., Jin, L., Yuan, Y., Han, Y., Zhao, Y., et al. (2019). Metal-free directed sp2-C–H borylation. Nature *575*, 336–340. https://doi.org/10.1038/s41586-019-1640-2.

42. Zhang, W., Zou, Z., Zhao, W., Lu, S., Wu, Z., Huang, M., Wang, X., Wang, Y., Liang, Y., Zhu, Y., et al. (2020). Integrated redox-active reagents for photoinduced regio- and stereoselective fluorocarboborylation. Nat. Commun. *11*, 2572. https://doi.org/10.1038/s41467-020-16477-1.

43. Oeschger, R., Su, B., Yu, I., Ehinger, C., Romero, E., He, S., and Hartwig, J. (2020). Diverse functionalization of strong alkyl C–H bonds by undirected borylation. Science *368*, 736–741. https://doi.org/10.1126/science.aba6146.

44. Renata, H., Wang, Z.J., Kitto, R.Z., and Arnold, F.H. (2014). P450-catalyzed asymmetric cyclopropanation of electron-deficient olefins under aerobic conditions. Catal. Sci. Technol. *4*, 3640–3643. https://doi.org/10.1039/C4CY00633J.

45. de la Torre, A., Kaiser, D., and Maulide, N. (2017). Flexible and chemoselective oxidation of amides to α-keto amides and α-hydroxy amides. J. Am. Chem. Soc. *139*, 6578–6581. https://doi.org/10.1021/jacs.7b02983.

46. Schwier, T., Sromek, A.W., Yap, D.M.L., Chernyak, D., and Gevorgyan, V. (2007). Mechanistically diverse copper-, silver-, and gold-catalyzed acyloxy and phosphatyloxy migrations: efficient synthesis of heterocycles via cascade migration/cycloisomerization approach. J. Am. Chem. Soc. *129*, 9868–9878. https://doi.org/10.1021/ja072446m.

47. Chen, H., Huang, Z., Hu, X., Tang, G., Xu, P., Zhao, Y., and Cheng, C.H. (2011). Nickel-catalyzed cross-coupling of aryl phosphates with arylboronic acids. J. Org. Chem. *76*, 2338–2344. https://doi.org/10.1021/jo2000034.

48. Pallikonda, G., and Chakravartya, M. (2016). Benzylic phosphates in Friedel-Crafts reactions with activated and unactivated arenes: access to polyarylated alkanes. J. Org. Chem. *81*, 2135–2142. https://doi.org/10.1021/acs.joc.5b02441.

49. Ackermann, L., Barfüsser, S., and Pospech, J. (2010). Palladium-catalyzed direct arylations, alkenylations, and benzylations through C–H bond cleavages with sulfamates or phosphates as electrophiles. Org. Lett. *12*, 724–726. https://doi.org/10.1021/ol9028034.

50. Xiao, J., Yang, J., Chen, T., and Han, L.-B. (2016). Nickel-catalyzed α-benzylation of arylacetonitriles via C–O activation. Adv. Synth. Catal. *358*, 816–819. https://doi.org/10.1002/adsc.201500822.

51. Dobson, C.M. (2004). Chemical space and biology. Nature *432*, 824–828. https://doi.org/10.1038/nature03192.

52. Chotana, G.A., Rak, M.A., and Smith, M.R. (2005). Sterically directed functionalization of aromatic C–H bonds: selective borylation Ortho to cyano groups in arenes and heterocycles. J. Am. Chem. Soc. *127*, 10539–10544. https://doi.org/10.1021/ja0428309.

53. Pabst, T.P., Quach, L., MacMillan, K.T., and Chirik, P.J. (2021). Mechanistic origins of regioselectivity in cobalt-catalyzed C(sp2)–H Borylation of Benzoate Esters and Arylboronate Esters. Chem *7*, 237–254. https://doi.org/10.1016/j.chempr.2020.11.017.

54. Roy, C.D., and Brown, H.C. (2007). Stability of boronic esters-Structural effects on the relative rates of transesterification of 2-(phenyl)-1,3,2-dioxaborolane. J. Organomet. Chem. *692*, 784–790. https://doi.org/10.1016/j.jorganchem.2006.10.013.